JOURNAL OF MATERIALS SCIENCE 15 (1980) 497–504

An investigation of novel methods of preparing dense, homogeneous, spinodally decomposable copper-nickel-iron alloys

ANNEMARIE STAUDINGER
Bell Telephone Laboratories, Murray Hill, New Jersey 07974, USA

The densification behaviour of four different powder metallurgical alloying techniques have been studied in two spinodally decomposable alloys, Cu 24.5–Ni 48.5–Fe 27.0 at. % and Cu 35.5–Ni 19.5–Fe 45.0 at. %. Three of the techniques involve variations in producing the alloy by the direct reduction of mixed oxides. The fourth technique uses mixed commercial elemental powders. Within short sintering times (2.5 to 4.5 h) at 1000° C, the first three techniques produced microstructurally homogeneous and very dense (96 to 99% theoretical density) alloys. Within the same times and temperatures, the fourth technique showed no increase in the as-pressed (~ 60%) densities. The difference in densification kinetics is believed to be due to the marked difference in specific surface area between alloy particles produced by the reduction of submicrometer oxide powders and atomized elemental powders ranging between 15 and 30 μm in size. The first three techniques are concluded to be useful and promising as means to produce homogeneous, high density Cu–Ni–Fe alloys.

1. Introduction

Cu–Ni–Fe alloys of a wide composition range, mainly within the two phase $\gamma + \gamma'$ region of the ternary phase diagram (see Fig. 1), are commercially important because they are known to be ductile permanent magnet materials [1, 2]. The solution-treated and homogenized alloys can withstand severe cold reduction and consequently can be formed into thin wire or tape, and also can be readily stamped and machined to produce a wide range of close tolerance parts. For example, one of the uses of Cu–Ni–Fe is in the magnetic recording of speech.

However, in the cast alloy, marked segregation can occur and the alloy cannot be satisfactorily hot worked due to the occurrence of hot-shortness. So it is normal to either produce small chill-cast ingots by vacuum melting or by using a neutral atmosphere, or to produce sintered bars using powders obtained by melting and atomization of the alloy [3]. These ingots and bars must then be homogenized at temperatures above the miscibility gap for several days. This step prepares the alloy for the final cold working and subsequent ageing within the immiscibility region to allow spinodal decomposition [4–6] in order to obtain optimum magnetic properties.

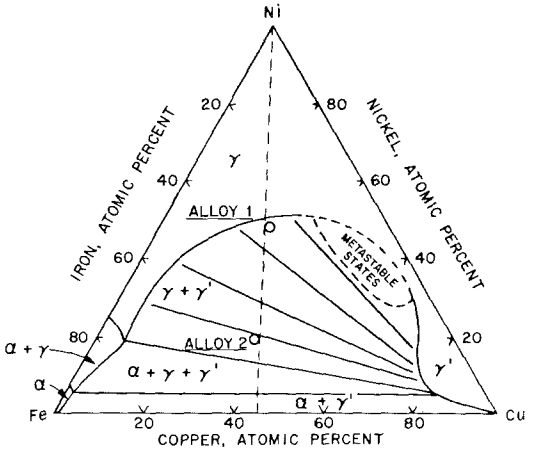

Figure 1 Cu–Ni–Fe 750° C isothermal equilibrium ternary phase diagram determined by Bradley [5]. It shows the positions of alloy 1 and 2 within the miscibility gap along a tie-line between the Ni-corner and the Fe–Cu side at 45 at. % copper.

0022–2461/80/020497–8$02.80/0

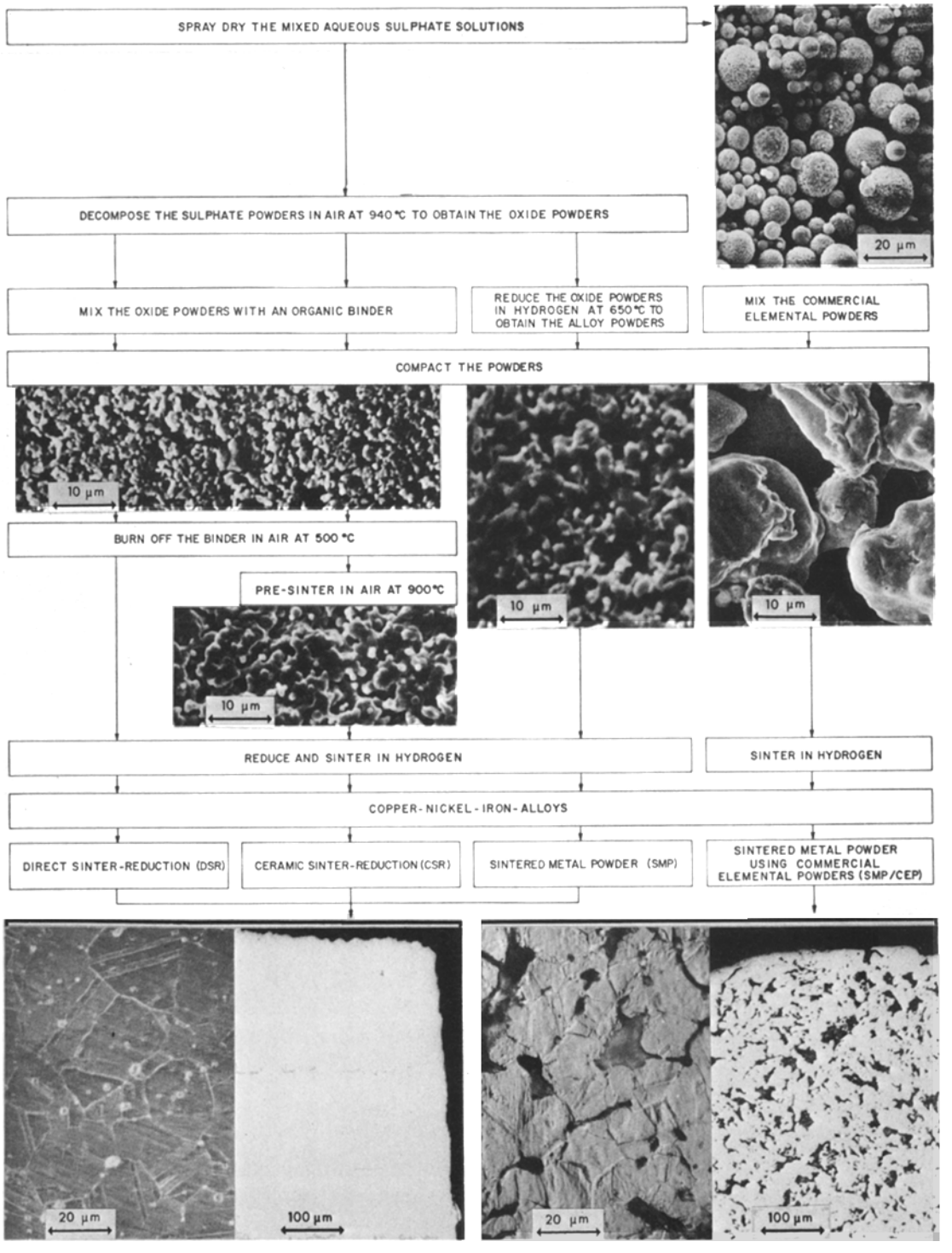

Figure 2 Flow diagram illustrating the steps involved in the preparation of DSR, CSR, SMP and SMP/CEP alloys. The two bottom left high and low magnification micrographs are typical microstructures of DSR, CSR and SMP samples; the two bottom right micrographs are typical of those of SMP/CEP samples, all sintered for 2.5 h at 1100° C.

In another paper [7], we described a method for metal and alloy pre-form preparation through the sinter-reduction of oxide powders, which produces very homogeneous and dense alloys. Utilizing the basic idea of this method, the present study is primarily concerned with the resulting densities and microstructures of Cu–Ni–Fe alloys obtained by varying the fabrication steps in this technique and comparing the properties of these alloys with those of alloys prepared by sintering the elemental powders. Two Cu–Ni–Fe compositions, Cu 24.5–Ni 48.5–Fe 27.0 at.% and Cu 35.5–Ni 19.5–Fe 45.0 at.%, have been studied.

2. Experimental procedure

Four different methods of producing the final alloy have been under investigation. These are summarized in the flow diagram of Fig. 2 and described below. The first method involves samples which have been directly sinter-reduced (DSR) in hydrogen using compacted oxides. The second method involves samples which have been ceramically sinter-reduced (CSR) in hydrogen using compacted and air-sintered oxides. The third method involves sintered metal powder (SMP) samples using compacted alloy powder, which has been obtained via pre-reduction of the oxide powder. The fourth method involves samples of mixed, compacted and sintered metal powder, using commercial elemental powders (SMP/CEP), which have been produced by atomization and have a particle size of about 30 μm.

The oxide powder starting materials for the DSR, CSR and SMP samples were prepared by spray-drying aqueous solutions of appropriate mixtures of Cu, Ni and Fe sulphates (see Table I). These were then decomposed in air for 8 h at 940° C to yield the oxide powders. The oxide powders for the SMP samples were reduced in hydrogen for 4 h at 650° C and those for the DSR and CSR samples were mixed with a binder, consisting of 10 wt% halowax dissolved in CCl_4.

TABLE I Sulphate and alloy compositions (g and at.%, respectively)

	Alloy 1	Alloy 2
$CuSO_4 \cdot 5H_2O$	207.1	299.7
$NiSO_4 \cdot 6H_2O$	431.3	172.8
$FeSO_4 \cdot 7H_2O$	253.9	423.1
Cu	24.5	35.5
Ni	48.5	19.5
Fe	27.0	45.0

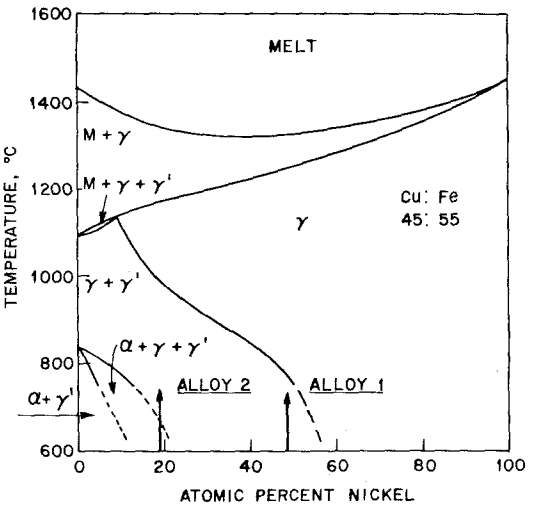

Figure 3 Schematic construction (using combined data by Bradley [5] and Köster and Dannöhl [8]) of the pseudo-binary equilibrium diagram showing the positions of alloy 1 and 2.

After the evaporation of the CCl_4, the powders were pressed into disc form at about 26 MPa on a hydraulic press. The binder was burned off in air at 500° C. The compacted oxide discs for the CSR samples were then sintered in air for 3 h at 900° C. The SMP and SMP/CEP samples were compacted into discs at about 100 MPa without the use of a binder.

DSR and CSR sinter-reductions and SMP and SMP/CEP sinterings were carried out at various times and temperatures in a glowbar furnace under flowing hydrogen. For optimum densification it proved beneficial to heat up the samples by the heat-up rate of the furnace. The sinter-reduction and sintering times given do not include the heat-up times. They are 25, 40, 50 and 70 min for the 700, 900, 1000 and 1100° C treatment temperatures. After sintering, all specimens were pushed out of the hot zone into the cool zone of the hydrogen furnace (which we call "air-quenching").

The compositions for the DSR, CSR and SMP samples in at.% determined by chemical analysis are given in Table I. For the SMP/CEP samples, appropriate amounts of elemental powders were mixed to yield the same compositions. Both alloys lie within the region of the miscibility gap on a pseudo-binary section along a tie-line between the Ni-corner and the Fe–Cu side at 45 at.% copper of the Cu–Ni–Fe ternary system. Fig. 1 shows the positions of the two alloys within the 750° C isothermal equilibrium phase diagram determined by Bradley [5]; Fig. 3 shows their positions within

a schematic construction (using combined data by Bradley [5] and Köster and Dannöhl [8]) of the pseudo-binary equlibrium diagram.

The densities of the two alloys produced by the four techniques are plotted as a function of sintering time and temperature and are shown in Figs. 4 to 7. These are immersion densities except for those with densities below 85% theoretical value. For the latter, corrected dimensionally measured bulk densities were obtained. Each data point represents the average of two samples. The theoretical densities for alloys 1 and 2 were calculated to be 8.64 and 8.47 g cm^{-3} respectively.

The microstructures of each alloy were examined by optical microscopy, scanning electron microscopy, including X-ray energy spectroscopy and X-ray diffractometry.

3. Results and discussion

Fig. 4 (alloy 1) illustrates that in the case of DSR, CSR and SMP samples and for a sintering time of 2.5 h, the resulting densities increase significantly up to 900° C (where an average density of ~91% is obtained). They then level off to the final densities of 96 to 97% at 1100° C. For the same sample types and under the same sintering conditions, quite similar densification behaviour is observed for alloy 2 in Fig. 5, where it is shown that the densities increase significantly up to 1000° C and an average density of ~96% is obtained. The density values then level off to the final densities of 99% at 1100° C. However, within

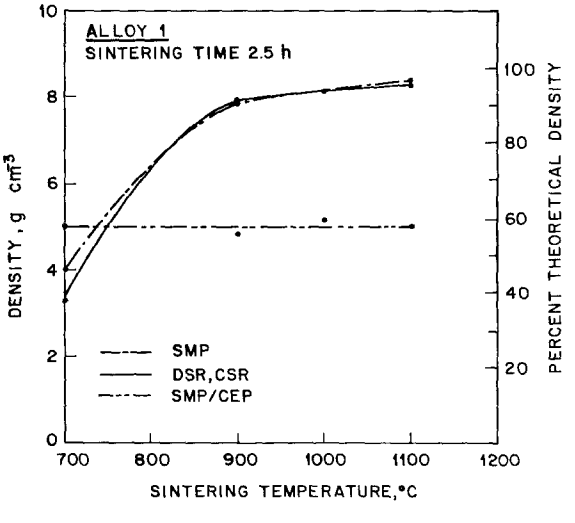

Figure 4 The density of alloy 1 samples for all four preparation techniques plotted as a function of sintering temperature for a sintering time of 2.5 h.

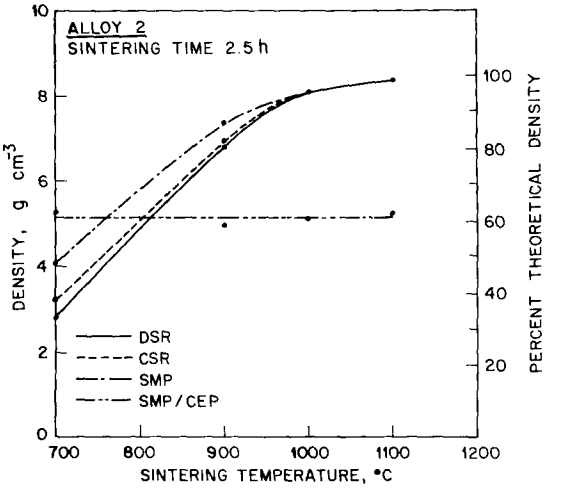

Figure 5 The density of alloy 2 samples for all four preparation techniques plotted as a function of sintering temperature for a sintering time of 2.5 h.

the given sintering times and temperatures no increase of the initial pressed density of the SMP/CEP samples (~ 60%) is observed for either alloy.

A comparison between Figs. 6 and 7 shows the densification kinetics to be slightly faster for alloy 1 than for alloy 2. At a sintering temperature of 1000° C, all DSR, CSR and SMP samples of alloy 1 densify within 0.5 h to greater than 90%, while about 2 h are needed for alloy 2 for the same densification. No significant increases in densities are observed at longer than 2.5 h; i.e. the increases between 2.5 h and 4.5 h at 1000° C range between 1.4 and 3.3% for DSR, CSR and SMP samples of both alloys. Again, no density increase is observed between the as-pressed and sintered states of SMP/

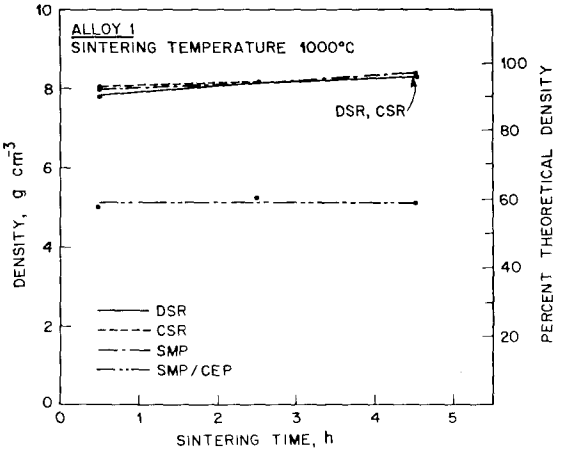

Figure 6 The densities of alloy 1 samples for all four preparation techniques plotted as a function of sintering time at 1000° C.

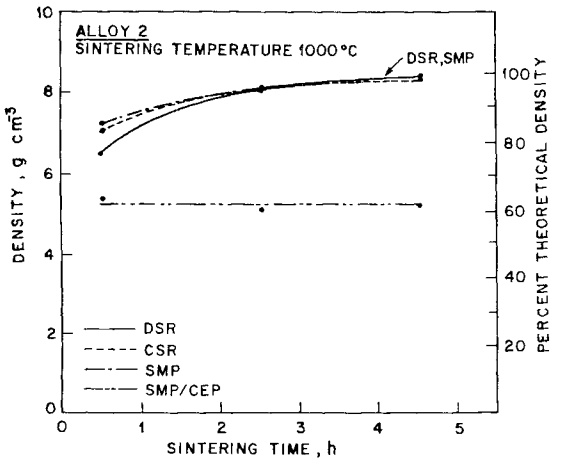

Figure 7 The densities of alloy 2 samples for all four preparation techniques plotted as a function of sintering time at 1000° C.

CEP samples of either alloy. The above results are summarized in Table II and III.

Optical microscopy revealed identical and very homogeneous microstructures for DSR, CSR and SMP alloy production techniques. Typical grain sizes for both alloys at 1000 and 1100° C are 20 and 25 μm, respectively. For example, Fig. 8a, b, c and d show unetched low magnification micrographs (exhibiting no detectable porosity) and etched high magnification micrographs of alloy 1 samples produced by DSR and SMP methods, respectively, and sintered for 2.5 h at 1100° C.

X-ray diffractometry confirms the optical microstructural results, i.e. the formation of the γ-phase has been completed (along with the onset of spinodal decomposition). This is shown in

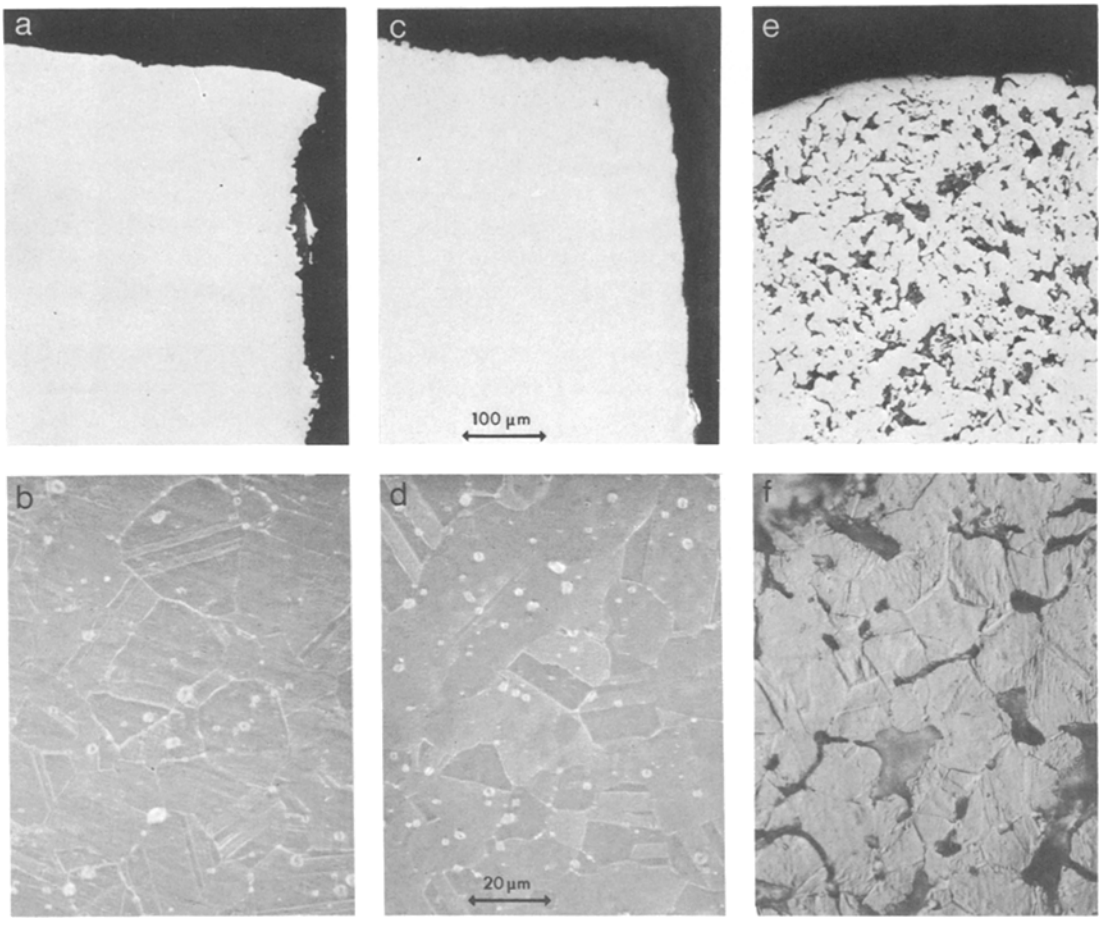

Figure 8 DSR, SMP and SMP/CEP samples sintered for 2.5 h at 1100° C. (a) DSR; unetched low magnification showing no detectable porosity; (b) DSR; etched high magnification showing a grain size of ~ 25 μm; the white dots are etch-pits; (c) SMP; unetched low magnification showing no detectable porosity; (d) SMP; etched high magnification showing a grain size of ~ 25 μm; the white dots are etch-pits; (e) SMP/CEP; unetched low magnification showing high porosity; (f) SMP/CEP; etched high magnification showing a grain size of ~ 25 μm.

TABLE II % theoretical density sintered for 2.5 h at different temperatures

Hydrogen sintering temperature (° C)	DSR		CSR		SMP		SMP/CEP	
	Alloy 1	Alloy 2	Alloy 1	Alloy 2	Alloy 1	Alloy 2	Alloy 1	Alloy 2
700	39.3	33.0	39.3	37.8	46.7	47.9	58.6	62 4
900	91.7	80.2	91.6	81.5	91.0	96.8	57.0	58.8
1000	94.3	95.5	94.8	96.0	94.3	95.5	60.8	61.1
1100	96.5	99.0	96.5	98.9	97.1	98.9	58.5	61.9

TABLE III % theoretical density sintered at 1000° C for different sintering times

Hydrogen sintering time (h)	DSR		CSR		SMP		SEM/CEP	
	Alloy 1	Alloy 2	Alloy 1	Alloy 2	Alloy 1	Alloy 2	Alloy 1	Alloy 2
0.5	90.7	76.8	93.3	83.2	92.9	85.0	58.3	63.2
2.5	94.3	95.5	94.8	96.0	94.3	95.5	60.8	61.1
4.5	96.0	98.8	96.2	97.9	97.2	98.8	59.0	61.7

Figs. 9 and 10 for DSR and SMP samples of alloy 1 and 2, respectively.

Microstructurally, the following has been observed in SMP/CEP samples: while almost complete interdiffusion and some sintering occurred in the samples of alloy 1 sintered for 2.5 h at 1100° C, incomplete interdiffusion and some sintering was observed in alloy 2. The interdiffusion behaviour is shown in the X-ray intensity profiles of Fig. 11a (alloy 1) and b (alloy 2). The matching optical micrographs for an SMP/CEP sample of alloy 1 can be seen in Fig. 8e, showing high porosity in the unetched low magnification micrograph and, in Fig. 8f, revealing the same grain size (~ 25 μm) as its DSR, CSR and SMP counterparts for the same heat-treatment conditions.

It is obvious that different preparation techniques are responsible for the varying densification properties observed in this study. It can be hypothesized that the reduction of specific internal surface area of a compact during heat treatment plays the primary role in the resulting sintered densities. For example, a comparison between the compacted powders (see Fig. 2) reveals submicrometer starting particles (therefore high specific surface area) for SMP, and ~ 15 to 30 μm particles

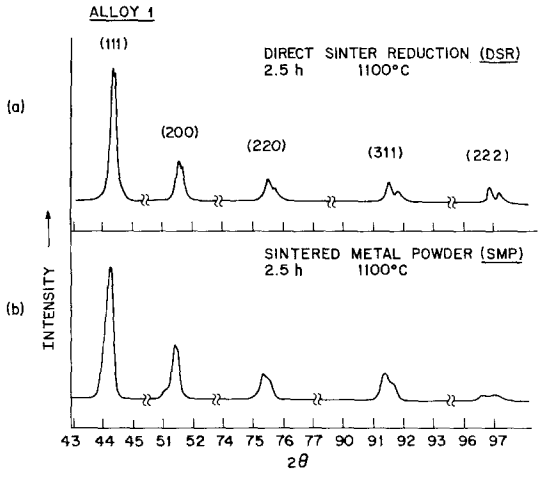

Figure 9 X-ray intensity as a function of diffraction angle 2θ of alloy 1 samples, sintered for 2.5 h at 1100° C. (a) DSR profile showing the completed formation of the γ-phase; (b) SMP profile showing the completed formation of the γ-phase and the onset of spinodal decomposition.

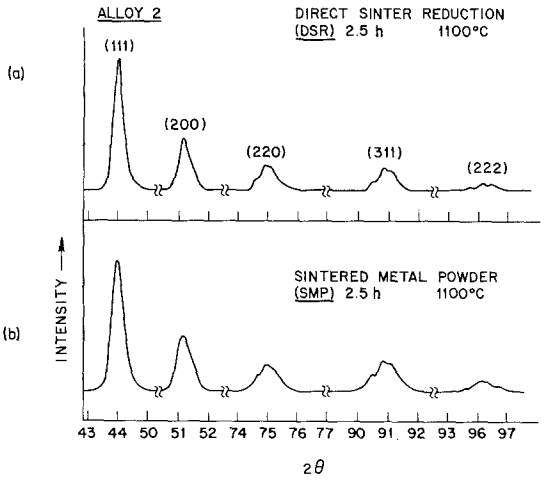

Figure 10 X-ray intensity as a function of diffraction angle 2θ of alloy 2 samples, sintered for 2.5 h at 1100° C. (a) DSR, and (b) SMP profiles both showing the completed formation of the γ-phase and the onset of spinodal decomposition.

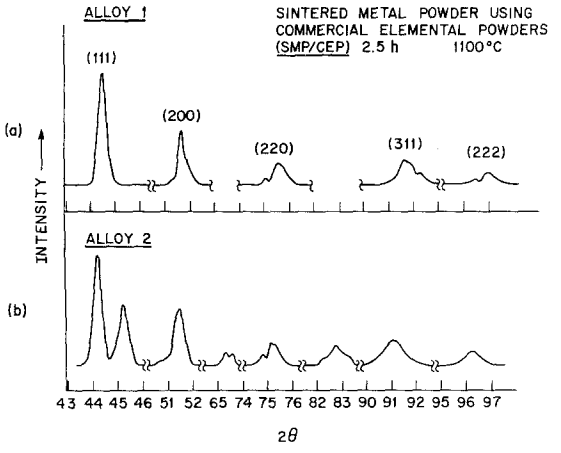

Figure 11 X-ray intensity as a function of diffraction angle 2θ of SMP/CEP samples, sintered for 2.5 h at 1100° C. (a) Alloy 1 profile showing almost completed homogenization; (b) alloy 2 profile showing incomplete homogenization.

(low specific surface area) for SMP/CEP preparation techniques.

Although SMP samples have been compacted under the same pressure as SMP/CEP samples, their starting density is about 20% lower. This gives SMP samples the additional advantage of greater pore mobility during sintering.

The DSR and CSR results can be explained in the same terms as the SMP results, the only difference being the starting density of the compact. This density can be assumed as even lower than the SMP starting density, since it is an oxide at this stage. For example, the hydrogen reduction from the oxide green density to the alloy without sintering (i.e. no changes in dimensions are to occur) would result in an alloy density of ~ 26%.

The faster densification properties of alloy 1 relative to alloy 2 in the temperature range of 700 to 1000° C cannot be attributed to the oxide reduction reaction, because the SMP samples exhibit the same trend as the DSR and CSR materials. Although the diffusion of nickel in iron is an order of magnitude slower than that of iron in nickel, an argument involving relative diffusion coefficients would only be warranted for SMP/CEP samples, for which all three constituents must travel considerable diffusion distances in each alloy in order to equilibrate. This is not the case for DSR, CSR and SMP samples where "pre-alloying" occurred due to the preliminary chemical mixing of the metal salts.

Consequently, the difference in kinetics may, for the most part, be attributed to the position of the two alloys in the ternary equilibrium phase diagram. Above ~ 780° C, alloy 1 is single-phase and, therefore, only small diffusion distances are necessary for homogenization during densification. Alloy 2, on the other hand, is two-phase up to almost 1000° C and the development of its equilibrium structure involves phase separation requiring longer diffusion distances than in alloy 1. For densification processes above 1000° C, where both alloys are single-phase, they exhibit similar densification behaviour.

4. Conclusions

Of the four methods investigated for producing Cu–Ni–Fe alloys, the DSR, CSR and SMP techniques, all of which involved first the production of the alloy as a mixed oxide, were significantly superior to the SMP/CEP process. The former alloys all exhibited excellent densification kinetics, whereas the SMP/CEP alloys showed no increase in density over the as-pressed value, and, consequently their microstructure was very porous. In contrast, the microstructure of the former alloys of both compositions was uniform and homogeneous with no evidence of the segregation that is the plague of cast Cu–Ni–Fe alloys.

It is, therefore, apparent that the DSR, CSR and SMP alloying methods are all superior to the technique of powder metallurgy or casting of Cu–Ni–Fe alloys currently employed. In particular, the DSR process is to be recommended because of its simplicity and consequent economic advantage.

Acknowledgements

The author wishes to thank M. Robbins, G. Y. Chin, D. W. Johnson, C. M. Preece, H. M. O'Bryan, V. G. Lambrecht and S. Mahajan for helpful discussions.

References

1. ALLOY DIGEST, Filing Code: Cu-105 Engineering Alloys Digest, Inc., New Jersey (1961).
2. R. M. BOZORTH, "Ferromagnetism" (van Nostrand, New York, 1951).
3. J. S. HIRSCHHORN, "Introduction to Powder Metallurgy" (American Powder Metallurgy Institute, Princeton, N.J., 1969).
4. J. W. CAHN, *Trans. Met. Soc. A.I.M.E.* **242** (1968) 166.
5. A. J. BRADLEY, *Proc. Phys. Soc. (London)* **52** (1940) 80.

6. E. P. BUTLER and G. THOMAS, *Acta Met.* **18** (1970) 347.
7. M. ROBBINS, A. STAUDINGER and S. SHABAKA, *J. Mater. Sci.* **15** (1980) 527.
8. W. KÖSTER and W. DANNÖHL, *Z. Metallk.* **27** (1935) 220.

Received 6 June and accepted 29 August 1979.